



Supplement of

Identifying airborne snow metamorphism with stable water isotopes

Sonja Wahl et al.

Correspondence to: Sonja Wahl (sonja.wahl@uib.no)

The copyright of individual parts of the supplement might differ from the article licence.

This supplement contains additional figures to the main publication. Figure S1 shows the control run of an empty wind tunnel experiment and the evolution of the meteorological variables due to motor heating. Figure S2 gives details about the established humidity-isotope calibration curves that are used to correct isotopic vapour data at low humidity. Figure S3 shows the observed change in vapour isotopic composition during the snow introduction period. The vapour change is better described by assuming equilibrium fractionation during sublimation than assuming no fractionation.

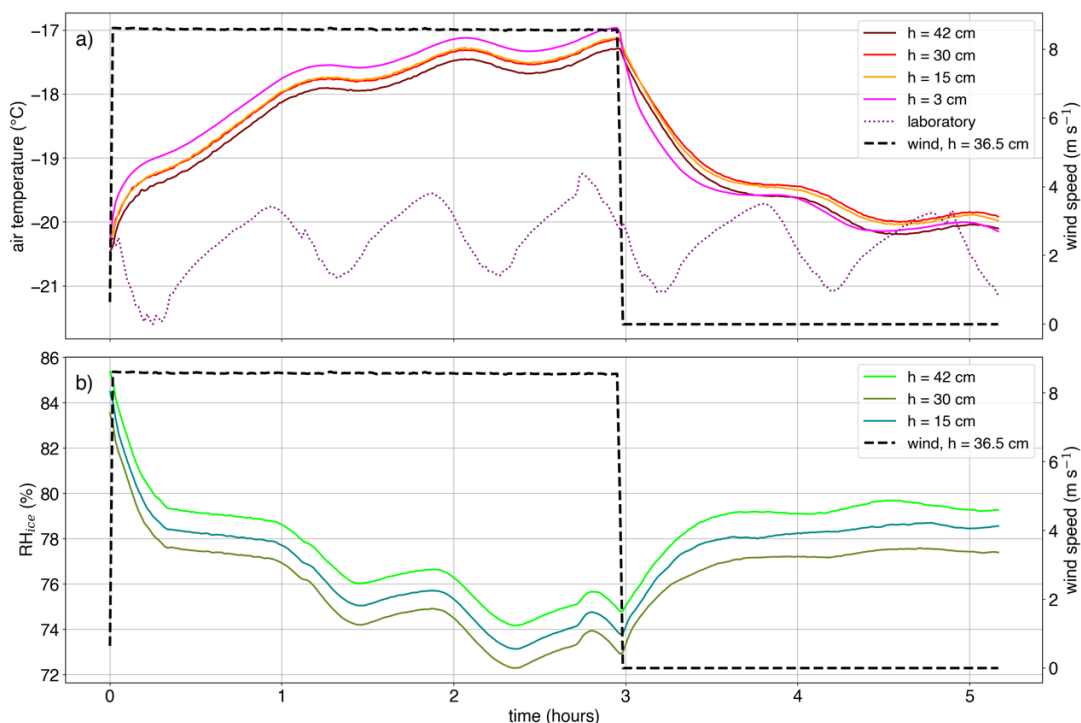
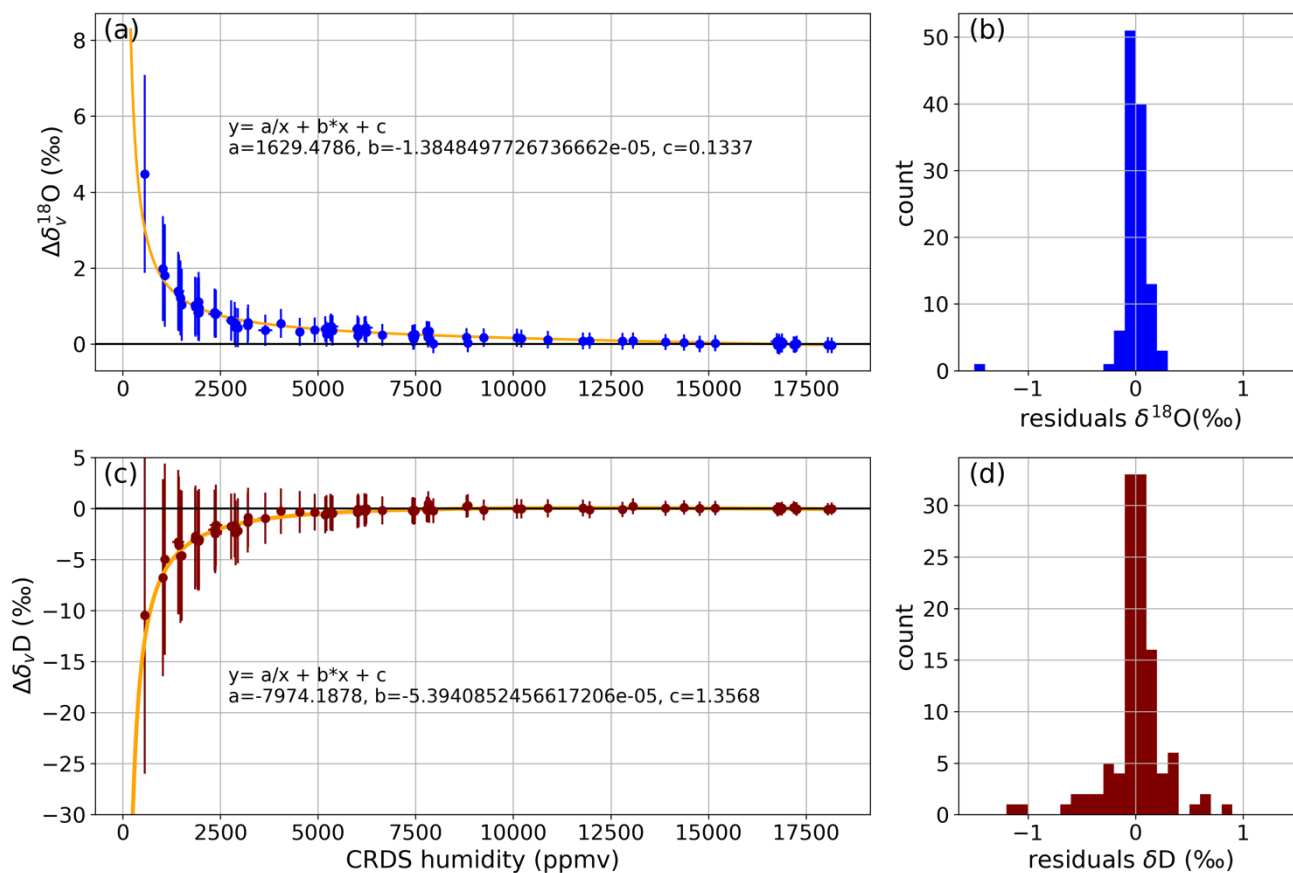


Figure S1: Control run of closed, sealed but empty wind tunnel With the initiation of the wind (wind speed = 9 m s^{-1}) the temperature inside the wind tunnel (averaged 1min, panel a) increases due to heating generated by the propeller motor which causes the relative humidity (RH_{ice} , averaged 1min, panel b) to decrease. After 3 hours the propeller was turned off (wind speed = 0 m s^{-1}) and the temperature inside the wind tunnel slowly decreased to laboratory room temperatures. The oscillations in the laboratory air temperature (dotted line, panel a) are the result of the climate control system regulating the laboratory temperature by episodic cooling.

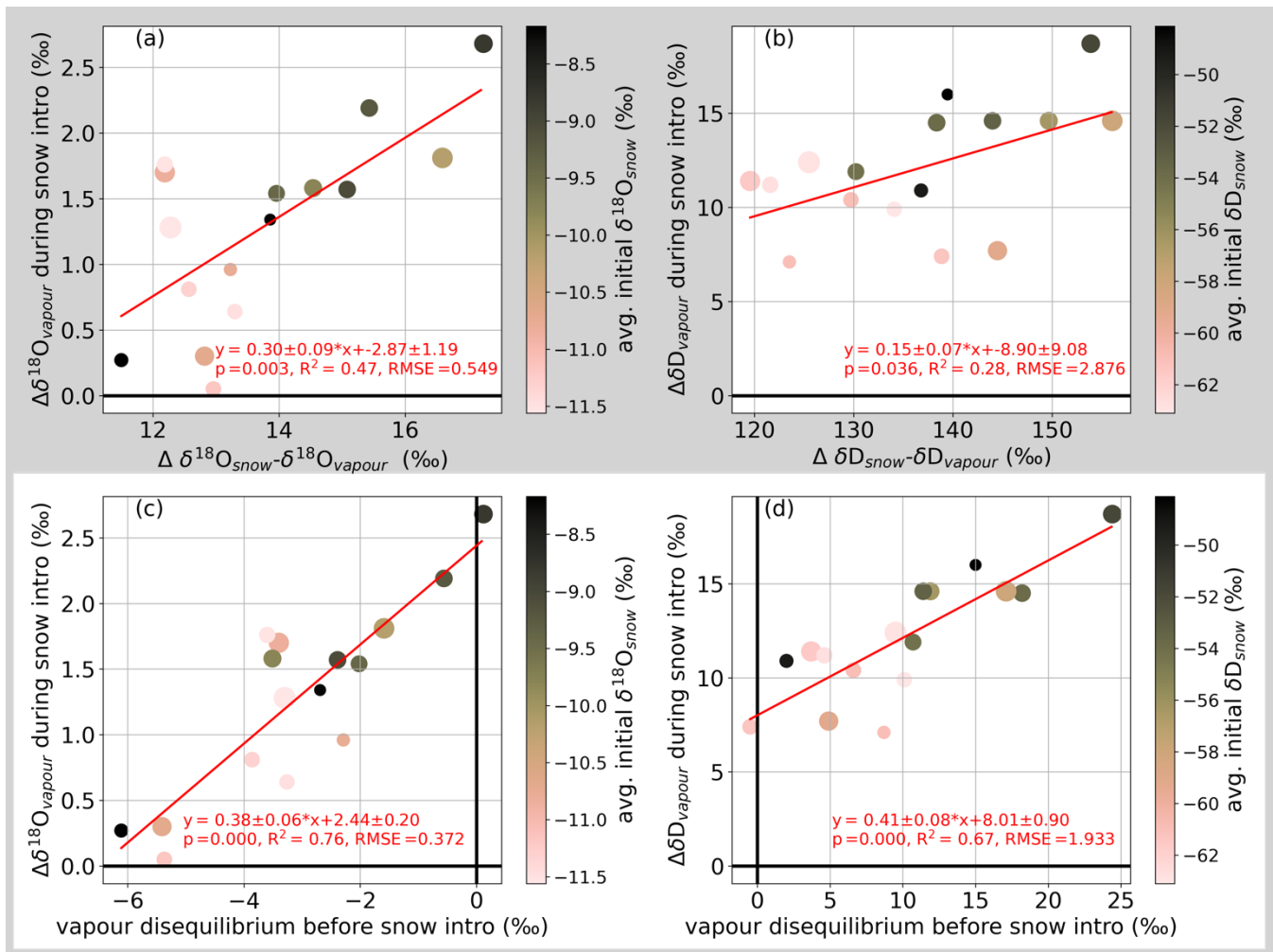
PCD Humidity-Isotope Calibration



15

Figure S2 Humidity-isotope calibration of CRDS instrument with PCD standard The 115 calibration run pulses are shown for $\delta^{18}\text{O}$ in (a) and for δD in (c). The data was normalised with the PCD standard water isotopic composition at 16821 ppmv averaged from ten calibration pulses with a standard deviation of 44 ppmv. The measured PCD value (mean \pm std) that was used for normalisation was $\delta^{18}\text{O} = -21.51 \text{‰} \pm 0.04 \text{‰}$ and $\delta\text{D} = -176.5 \text{‰} \pm 0.04 \text{‰}$ which was very similar to the ambient vapour isotopic composition during the experiments. Orthogonal best fits to $y = \frac{a}{x} + b \cdot x + c$ (Weng et al., 2020) are shown as orange lines and the best-fit parameters are given in panels (a) and (b). Histograms of the residuals to the fit are shown in (c) for $\delta^{18}\text{O}$ and in (d) for δD . The residuals are normally distributed around zero which supports the quality of the fitting routine. All vapour data has been corrected with this correction function.

25



30 **Figure S3 Change in vapour isotopic composition during snow introduction is better described assuming isotopic fractionation during sublimation** The change in vapour isotopic composition during the snow introduction period is calculated from the 3 min-averaged vapour data of the 16 experiments in May. The change in $\delta^{18}\text{O}$ is given on the y axes in (a) and (c) and for δD in (b) and (d). The colour code represents the initial snow isotopic composition. The changes are plotted against the difference between initial snow and initial vapour isotopic composition before the snow introduction in the upper, grey panels (a&b). In the lower panels, it is plotted against the calculated vapour disequilibrium assuming equilibrium fractionation during sublimation. Linear least-square fits are given with fit statistics in each panel. The mix of sublimated snow and initial vapour when accounting for isotopic fractionation during sublimation is a better predictor for the observed variability in the vapour signal during snow introduction than the mere difference of snow and initial vapour (i.e. assuming vapour from snow sublimation has the same isotopic composition as the snow).

40 References

Weng, Y., Touzeau, A., and Sodemann, H.: Correcting the impact of the isotope composition on the mixing ratio dependency of water vapour isotope measurements with cavity ring-down spectrometers, *Atmospheric Measurement Techniques*, 13, 3167–3190, <https://doi.org/10.5194/amt-13-3167-2020>, 2020.